Article

Diamond as Insulation for Conductive Diamond—A Spotted Pattern Design for Miniaturized Disinfection Devices

Manuel Zulla [1,†], **Vera Vierheilig** [1,†], **Maximilian Koch** [2,*], **Andreas Burkovski** [2], **Matthias Karl** [3] **and Stefan Rosiwal** [1]

[1] Material Sciences Division, Friedrich-Alexander-Universität Erlangen-Nürnberg, 91058 Erlangen, Germany; manuel.zulla@fau.de (M.Z.); vera.vierheilig@fau.de (V.V.); stefan.rosiwal@fau.de (S.R.)

[2] Microbiology Division, Department of Biology, Friedrich-Alexander-Universität Erlangen-Nürnberg, 91058 Erlangen, Germany; andreas.burkovski@fau.de

[3] Department of Prosthodontics, Saarland University, 66421 Homburg, Germany; matthias.karl@uks.eu

[*] Correspondence: max.koch@fau.de; Tel.: +49-09131-85-28090

[†] These authors contributed equally to this work.

Abstract: Boron-doped diamond (BDD) electrodes are well known for the in situ production of strong oxidants. These antimicrobial agents are produced directly from water without the need of storage or stabilization. An in situ production of reactive oxygen species (ROS) used as antimicrobial agents has also been used in recently developed medical applications. Although BDD electrodes also produce ROS during water electrolysis, only a few medical applications have appeared in the literature to date. This is probably due to the difficulties in the miniaturization of BDD electrodes, while maintaining a stable and efficient electrolytic process in order to obtain a clinical applicability. In this attempt, a cannula-based electrode design was achieved by insulating the anodic diamond layer from a cathodic cannula, using a second layer of non-conducting diamond. The undoped diamond (UDD) layer was successfully grown in a spotted pattern, resulting in a perfectly insulated yet still functional BDD layer, which can operate as a miniaturized flow reactor for medical applications. The spotted pattern was achieved by introducing a partial copper layer on top of the BDD layer, which was subsequently removed after growing the undoped diamond layer via etching. The initial analytical observations showed promising results for further chemical and microbial investigations.

Keywords: biocompatible diamond; carbon insulator; boron-doped diamond; BDD; disinfection; applied electrochemistry; diamond for health; diamond for environment; diamond coating

1. Introduction

Boron-doped diamond (BDD) electrodes are well known in the field of electrochemical advanced oxidation processes (EAOP). The possibilities for BDD applications seem endless, whenever chemical and mechanical robust surfaces or special electrolytic characteristics are needed. Diamond-coated electrodes have the potential to be more cost-effective, easily up-scalable, sustainable and a robust alternative to common electrode materials for disinfection purposes. Recent research showed a broad application list, e.g., decontaminating drinking water or wastewater [1–3], electrolytic preparation in organic or inorganic synthesis [4–9] or sensor technology [10]. In addition to these novel developments, BDD electrolysis has already arrived in industrial format, for example, in wastewater treatment (e.g., Clearfox DiOx, Bayreuth, Bavaria, Germany). Despite a host of beneficial properties of BDD electrodes, versus common electrode materials, their medical use has been poorly examined. The in situ production of strong oxidants mimics body-own defense mechanisms or produces the end products of mechanisms stimulated by bactericidal antibiotics [11]. Hence, the transfer of BDD as an ROS producing technology to the medical field seems inevitable [12]. Especially given that single and multiple resistant strains are on the rise. Nevertheless, only few approaches have arisen to date. Most of them are associated with

dental disinfection or related applications such as biofilm removal from infected areas, root canal obturation or dental bleaching [12–19].

Transferring research into industrial applications is often a struggle with "upscaling" from laboratory to industrial size. Vice versa, technologies for medical applications often undergo a miniaturization process. In the case of BDD electrodes, Ochiai et al. [20] demonstrated a disinfecting effect in bacterial suspension and suggested a dental application. However, the use of a tungsten-based BDD anodes remain questionable, at least in medical applications, due to the toxicity of tungsten. In the context of a root canal application, the general size of the presented electrode was too large for the root canal and the design was not ready for a clinical application. Previous work in the field of CVD diamond demonstrated that thin wires can be coated with diamond, matching the size requirements for root canal treatment [21,22]. In a new approach, further development in this field was achieved [13,14,18] by using an array of flexible BDD wires with a thickness of 200 µm, based on niobium, and insulated with a Teflon-coated PE-UHMW thread.

Still, the overall design was not applicable in a preclinical in vivo experiment. The construction was fragile and there was no option for an automatized supply for the electrolyte. To meet these tasks, the aim was a syringe-based design, which was implemented in the next prototypes for further preliminary and preclinical tests [17]. The insulating spacer material for the BDD electrodes was polymer-based (Plasti Dip, Plasti Dip Europe GmbH, Schwerin, Germany) and handcrafted in a spiral or droplet shape (Figure 1). The goal for a prototype design was an approximate size of 250 µm in outer diameter, limited by the specifications of apical orifices being 300–500 µm after preparation in root canal treatment [23]. The prototype has to leave enough space for an optimal irrigant exchange in the apical lumen of a root canal. Therefore, cannula gauges of 31 (261 µm outer diameter, 133 µm inner diameter) or higher are relevant for future development. The size of the anode and the insulator thickness are limited by the inner diameter of the cannula. To ensure an applicable electrolyte flow between anode and cathode, the insulator had to leave a canal for an electrolyte flow.

Figure 1. Polymeric insulation of boron-doped diamond. (**a**) BDD-coated Nb wire (200 µm, insulation layer 150 µm) insulated by a spiral-shaped polymeric gum insulator. (**b**) Droplet-insulated BDD-coated Nb wire (50 µm, insulation layer 10 µm) inside an endodontic cannula (250 µm).

In the preliminary work, the polymeric gum ensured a flexible and secure electrical insulation from the cannula, without impeding electrolyte flow. It left a maximized electrode surface area, with the lowest distance between BDD anode and the inside of the cannula as a steel cathode. The resistance of the polymer was measured as being over the limit (commercially available multimeter), even at a layer thickness of around 10 µm.

In addition to the mentioned advantages of polymeric insulation, some drawbacks must be addressed in the further development of the electrode array. The main disadvantage is the difficulty of executing the selective coating of BDD wires in a spiral or droplet shape. Another drawback is a possible detachment of the polymer, leaving a presumably non-biocompatible polymer inside the site of action. The thickness of the niobium wire, a polymeric insulation layer in the same dimensions and the wall thickness of the steel cannula already limits the applicability of the shown device (compare Figure 1a, Ø >> 500 µm) for root canal treatment. A partial insulation of the wires with smaller diam-

eter (50 μm, insulation layer 10 μm) was possible (Figure 1b), but it was not applicable for a reliable production.

For further development of the prototype, the aim was to design a reliable and polymer-free insulation process for a dimensionally reduced electrode with a determinable active surface. Ideally, the insulation can directly be integrated into the diamond-coating process. The resulting BDD wire should show properties without major cutbacks in flexibility and insulation, compared to the polymeric approach. However, progress is expected in controlling the insulation layer thickness and the size of the electrolytically active surface while excluding the detachment of the insulator.

The diamond semiconductor used in this study was based on doping the diamond lattice with boron atoms. The most logical insulation appeared to be undoped diamond (UDD) itself, as it is a perfect electrical insulator. The coating may work as an appending step during prototype manufacturing and fits exceptionally well with all the above-mentioned primary requirements. The concept to use UDD as insulator for BDD on such scale is known as "all-diamond microelectrode" in the literature [24–26]. The major challenges are represented in generating a controllable process for a selective coating of BDD with UDD. The resulting double diamond laminate (DDL) should also contain a zone without any coating, to ensure a safe and stable electrical connection (Figure 2). Therefore, about 50% of the BDD surface remain accessible for the electrolyte and potential e-lectrochemical reactions.
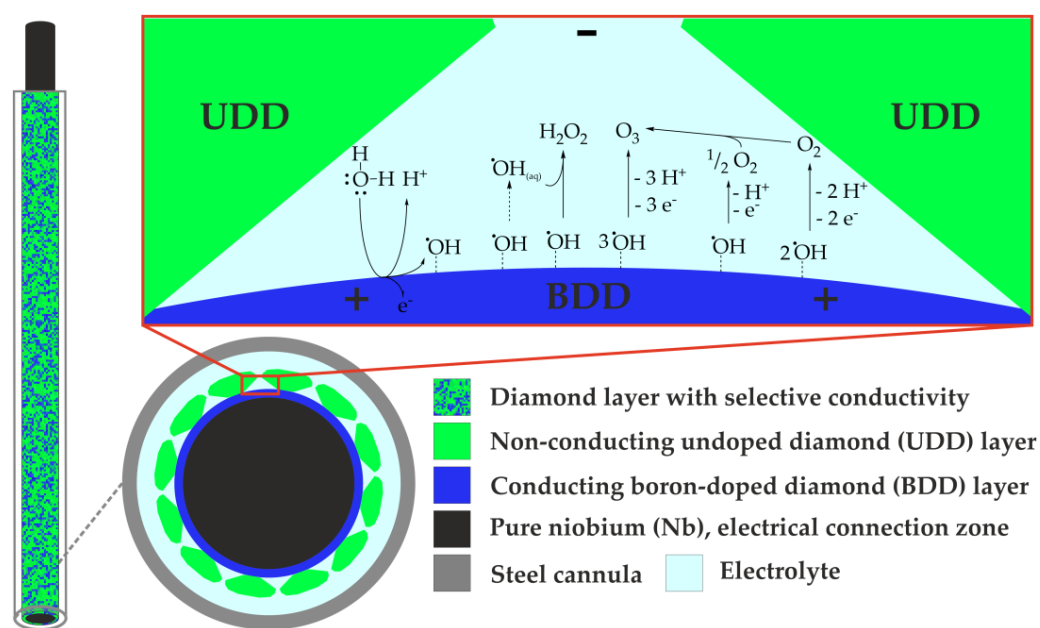

Figure 2. Schematic view of a niobium wire coated with boron-doped diamond (BDD) and insulated by undoped diamond (UDD). The partial UDD layer may lead to a perfect insulation with minimized spacing between the BDD anode and the steel cathode. An excerpt of possible anodic reactions is shown.

2. Materials and Methods

2.1. Conductive Diamond Coating of Niobium Wires

The substrate (niobium wire of 50 μm in diameter) required for the diamond coating was obtained from Plansee Metall GmbH (Reutte, Austria). The coating was performed in a Hot-Filament Chemical Vapor Deposition (HFCVD) chamber, in a hydrogen–methane gas atmosphere. Trimethyl borate (TMB) was added as the dopant for a conductive diamond layer. The gas phase consisted of 1000 mL/min hydrogen, 16 mL/min methane and 0.15 mL/min TMB. The coating procedure was performed at approximately 800 °C for 6 h with a chamber pressure of 2 mbar. This resulted in a 1–2 μm thick conductive diamond layer (first coating: BDD), which featured all desired electrochemical properties [27]. All deposited layers were analyzed with a scanning electron microscope and energy-dispersive

X-ray spectroscopy. Manual cutting, with the help of a side cutter, provided the cross-sections required for the analysis.

2.2. Spotted Copper Deposition (SCD) as Intermediate Layer

In a simple galvanic setup (Figure 3), the BDD-Nb wire was partially coated with Cu; (+) BDD-Nb electrode, (−) BDD niobium wire (sample, working electrode) (Figure 3). A current of 50 mA, at a voltage of around 1.5 V, was applied for 2–10 s. A copper (II) sulfate pentahydrate solution (20 g/L) was used as an electrolyte.
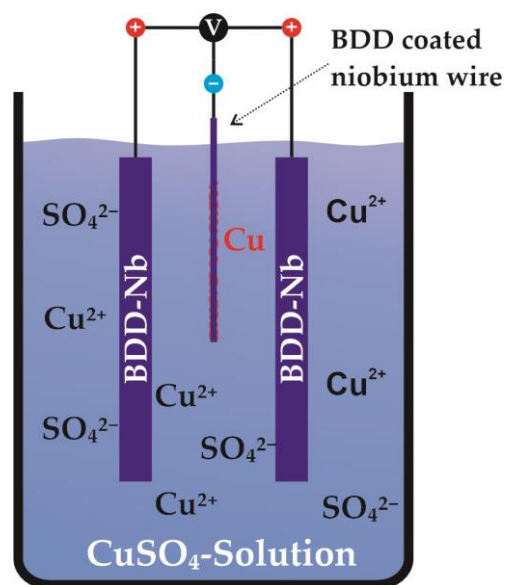

Figure 3. Scheme of the copper deposition in an electrolytic cell with BDD-Nb sheet counter electrodes (+) and the BDD coated niobium wire as working electrode (−) in a copper sulphate electrolyte.

2.3. Non-Conductive Diamond Coating of BDD/Cu/Niobium Wires

The deposition procedure was almost analogous to 2.1, except that no TMB-dopant was present. The gas phase consisted of 1000 mL/min hydrogen and 16 mL/min methane. The deposition time was varied from 5 h to 15 h in order to investigate different porosities with increasing UDD layer thickness. Subsequently, the deposition time was extended to 20 h for the final prototype, as previous coatings did not guarantee a reliable insulation. The 20 h deposition resulted in a UDD layer thickness of around 3–4 µm.

2.4. Electrochemical and Acidic Etching of Copper

The copper was removed after the UDD layer deposition by a 2-step etching process. First, the positively charged DDL was reacting with a negatively charged BDD electrode in a simple electrolyte setup with distilled water as electrolyte. Then, 10 V were applied for 2 min (electrochemical etching). To remove any copper residues, a second etching step (nitric acid 20%, hypochlorous acid 20%, 1:1) was added. The acidic etching procedure was performed twice. The wires were cleaned in an ultrasonic bath with distilled water between the single etching steps.

2.5. Prototype Design and Manufacturing Process

The experimental setup was designed to be as simple as possible to verify the functionality of the DDL. The DDL was inserted into a steel cannula and guided outward at an elongated recess in the plastic adapter of the cannula. The cone of a syringe filled with electrolyte was connected to the medical cannula. The steel cannula was contacted negatively via a clamping contact. The exposed end of the DDL was contacted positively. The prototype design was based on the work of [17]. A schematic manufacturing route from the bare Nb-wire to the prototype is shown in the Supplementary Material (see Figure S1).

2.6. Analysis of Oxidant Production

The manufactured prototypes (DDL) were determined to be operational as a function of oxidant production. A potential of 5–15 V was applied to the DDL while it was rinsed (10 mL/min) with demineralized water (<50 µS/cm). Single droplets were then collected with semiquantitative hydrogen peroxide test strips (Quantofix® Peroxid 25, Macherey-Nagel GmbH Co. KG, Düren, Germany).

3. Results

The aim for this work was to find a reliable and controlled process for a partial insulation of a low-diameter BDD-coated niobium wire. The processed wire had to maintain equal electrochemical properties compared to the electrochemical properties of the former polymeric wire.

3.1. Electrochemical Deposition of Copper as Intermediate Layer

The partial coating of the conductive BDD with non-conductive UDD required an intermediate step, because HFCVD coatings are "unspecific" (diamond on diamond in this case) and normally produce dense layers. The solution for this challenge was to apply a selective intermediate copper layer that inhibited adhesive diamond growth during the second coating step (UDD top-layer) to ensure that the electrochemically active BDD layer was not blocked completely (Figure 4).
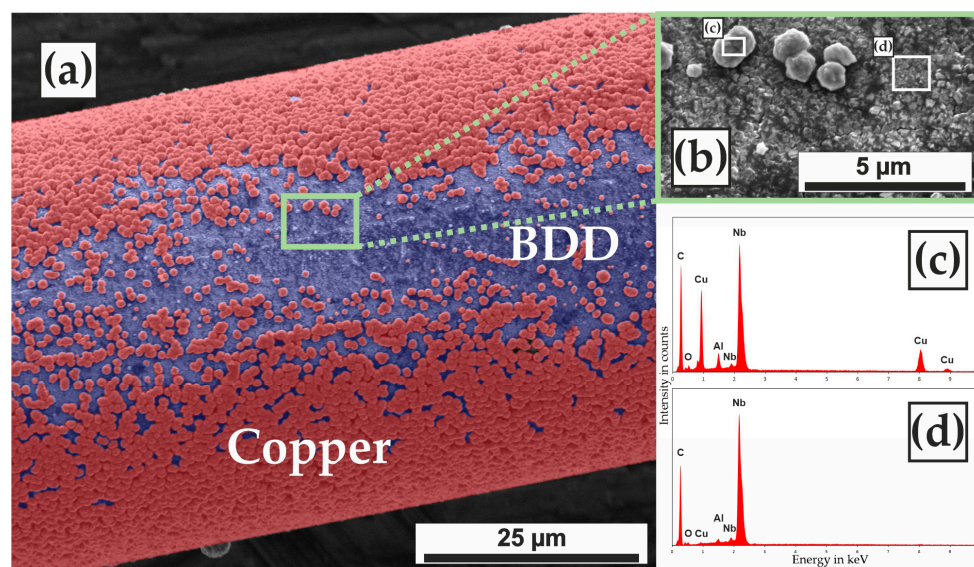

Figure 4. Artificially colored SEM image of the electrochemically deposited copper particles (colored red) on a BDD-coated (colored in blue) niobium wire after the SCD (**a**). Sections of the SEM image (**b**) are used for EDX analysis with (**c**) and without (**d**) copper precipitation. The raw SEM image is provided in the Supplementary Material (see Figure S2).

The agglomerate-like copper precipitates showed an unequal distribution over the BDD surface. The copper depositions appeared to follow a gradient. While the deposits were only found sporadically in the center, the peripheral areas tended to overgrow, which were directly facing the positively charged BDD-Nb counter electrodes during the SCD (compare 2.2).

3.2. Double Diamond Laminate

The concept of a non-polymer-based insulation of the BDD niobium wire in a steel cannula is shown in Figure 2. The realization and its outcome are shown in Figure 5 in a cross-section of the DDL.
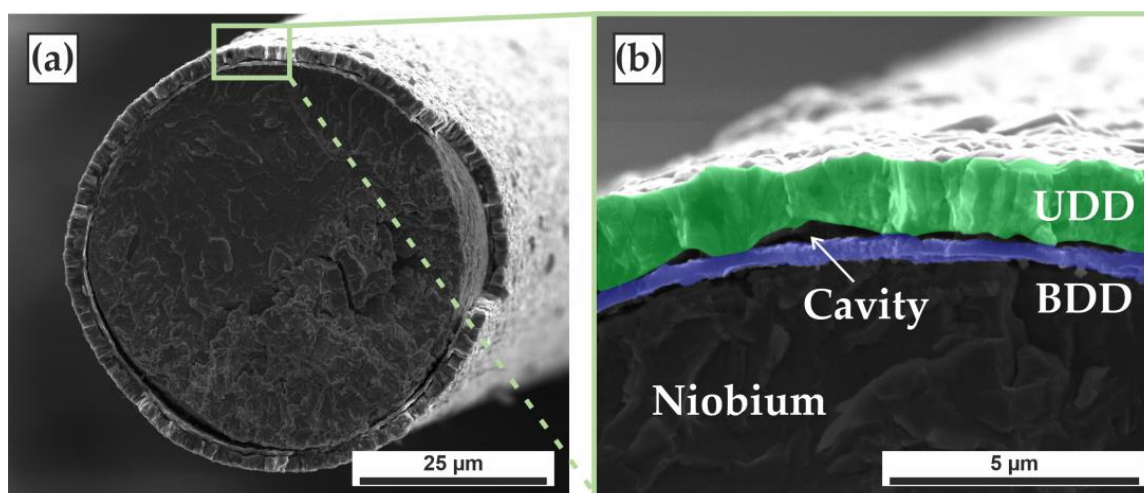
Figure 5. SEM image of the niobium wire cross-section after BDD and UDD coating. The copper interlayer has already been removed. (**a**) Overview of the double diamond laminate; (**b**) enlarged view of the niobium–diamond transition with artificial coloring. The BDD (1 μm thick, in blue) layer lies flush on the niobium substrate. The overlaying UDD (3 μm thick, in green) is not grown together and shows cavities with free BDD. The raw SEM images are provided in the Supplementary Material (see Figure S3).

The niobium wires were able to be coated with two different layers of CVD diamond. Both coatings showed sufficient bonding to its substrate. The initial layer (colored in blue) was the 1 μm thick boron-doped CVD diamond (Figure 5b). The BDD was overlaid by the UDD (green, ~3 μm) in the second CVD coating process. At the interface of the two diamond layers, both homogenous transitions and highly fissured areas can be seen. The latter represents cavities between those layers. The cavities exhibit irregular contours and morphologies from which a pattern cannot be derived from. Those represent relics of the successful partial deposition of copper on the BDD layer (Figure 4a), which was subsequently removed after the UDD coating by an etching process.

3.3. Formation of Active BDD Sites as a Spotted Pattern

As the thickness of the UDD layer increased with time, the primary coating surface (BDD + Cu) became superficially sealed. The insular copper precipitates (Figure 4) led to a partial UDD coating on top of the BDD layer, resulting in electrochemical active sites within the non-conductive diamond top layer (Figure 6).

The comparison between 5 h and 15 h coating time was mainly expressed by the progressive closing of pores, due to higher layer thickness over time. Configuring a disinfection device, without the need for additional insulation, became possible by the realization of these specific layer characteristics and subsequent removal of the copper interlayer. Although the thicker UDD layer almost covered the whole wire, most of the BDD layer was still accessible to the electrolyte due to the remaining pores in the UDD layer. Application tests showed that the UDD layer must be at least 3 μm thick to ensure sufficient insulation properties to insulate also large exposed BDD areas (Figure 6c,d). Figure 6d also gives a good impression about the different diamond morphologies. The UDD had columnar grown crystals with diamond facets up to 1–2 μm. The BDD layer, on the other side, showed a nanocrystalline diamond layer, which cannot be further resolved by the SEM images.
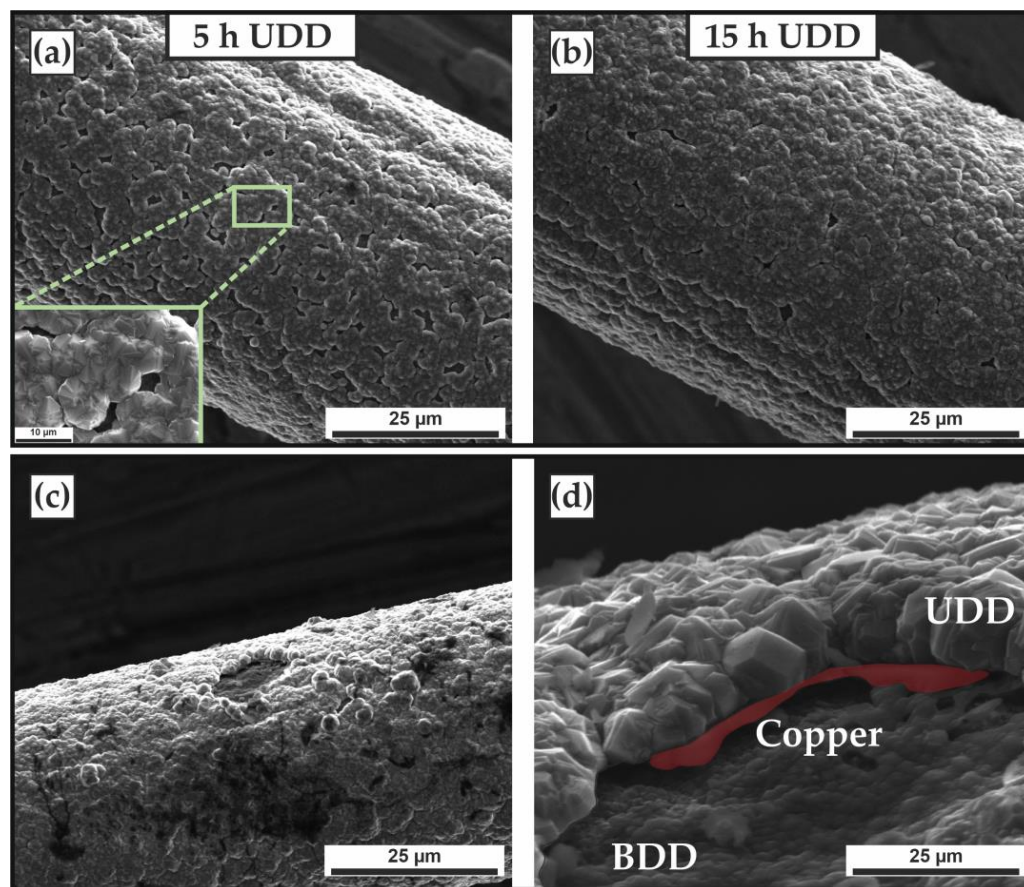
Figure 6. SEM image of the growth of the UDD layer on the BDD–Cu-coated niobium wire, after 5 h (**a**) and 15 h (**b**) of HFCVD processing time. The pores shrink with increasing coating time. Panel (**c**) and (**d**) show an enlarged pore after one etching step, with a residual copper layer (**d**) between BDD and UDD. The residual copper layer is artificially colored. The raw SEM images are provided in the Supplementary Material (see Figure S4). EDX spectra of all layers are presented in the Supplementary Material (see Figure S5). Raman spectra of UDD and BDD layers are presented in the Supplementary Material (see Figure S6).

3.4. Oxidant Production Screening with DDL

An experiment, based on the production of hydrogen peroxide with a DDL anode and a steel counter electrode, was used to determine the general ability to produce oxidative species. The tests showed different concentrations of hydrogen peroxide production. With increasing applied voltage and the resulting currents, there was a continuous increase in the hydrogen peroxide concentrations up to 30 mg/L (at 15 V, 20 mA) in distilled water, per droplet analyzed. The electrochemically active zone corresponded to 3 cm of the coated wire's length. Due to the DDL design, roughly 80% of the BDD area ($\sim$0.075 cm^2) was electrochemically active. The applied voltages resulted in currents within the range 1–20 mA, which, in turn, led to current densities of 0.01–0.27 A/cm^2. Although current densities up to 0.5 A/cm^2 were realized, a delamination resulting from high current densities could not be detected, presumably prevented by the short experimental timeframe.

4. Discussion

Due to the combination of different coating strategies (CVD, SCD), it was possible to use DDL as a disinfection unit within a steel cannula and without the need for additional insulation.

4.1. Diamond as Insulation and Electrochemical Active Site

Diamond is well known for its insulating properties (band gap 5.47 eV at 300 K). However, the boron doping of diamond enables unique electrochemical properties featuring the hydroxyl radical production. It seems logical to take advantage of both capabilities when it is possible to integrate it into an applicable electrode configuration. The presented approach is a further development of the work from Koch et al., Böhm et al. and Göltz et al. [13,14,16–19]. This approach eliminates the need for an insulation containing polymers, which can lead to potentially undesirable by-products [28]. In addition, the approach also safely integrates an oxidative component (in this case, the DDL) into almost arbitrarily large steel cannulas. This means that it is possible to equip a cannula as thin as a fine pen needle (200 μm) with a disinfecting device based on BDD technology.

The SCD serves solely to block specific diamond growth areas for the second CVD process. Copper was already used in the past for controlling CVD diamond growth in specific areas on silicon substrate [29], as copper is a non-carbide forming element. The electric field build-up between the wire (cathode) and two planar BDD anodes facing each other is responsible for the uneven distribution of copper particles during the electrochemical deposition step. All other sites, exposed BDD in this case, will be overgrown with UDD and will be electrochemically inert (insulation). In turn, after the acidic dissolution of copper, the former copper-covered BDD areas will be exposed and provide the basis for EAOPs in the subsurface of the DDL.

4.2. Introduction of a More Realistic Model of DDL

Considering the fundamental idea of the DDL approach and the results of this work, the following model can be established (Figure 7).
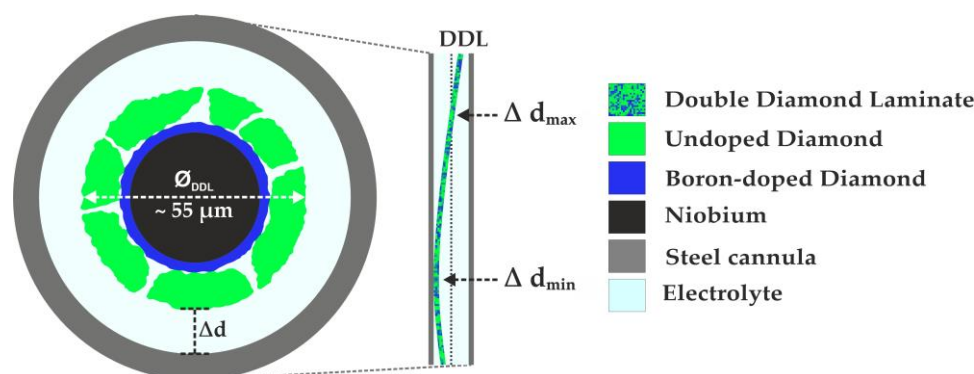

Figure 7. Double Diamond Laminate in 2D (horizontal) and 2D (vertical) with the corresponding steel cannula and electrolyte. The dominance of open porosity within the UDD is shown. A total of 80% of the BDD surface represented in the model is still accessible for the electrolyte. The vertical section shows that the DDL is not concentrically placed in the cannula, resulting in a variable electrode gap Δ d. The representation is not true to scale.

Approximately 20% of the BDD surface area was directly overgrown with UDD (Figure 7). The active surface was increased significantly in comparison to the approach of Koch et al. [17]. In that approach, the polymer-based insulation blocked roughly 50% of the electrochemical active surface and, therefore, led to a potentially lower oxidative performance. The appearance of the karst cave-like structure, developing between both diamond layers, was highly dependent on the SCD and the resulting spotted pattern. It suggests the use of a cylindrical anode to create a more homogenous distribution of copper spots than achieved in this work (see Figure 4). The crevice-like structures, due to the copper intermediate layer, below and within the UDD layer still allowed the electrolyte to reach the BDD surface, where it was electrochemically activated. The approach presented in this work formed a partial insulated anode with a diameter of ~55 μm. The active surface and the insulation layer thickness were controllable by the process presented in this work.

Furthermore, the distance between anode and cathode was reduced to a minimum distance of 3–5 μm compared to 10 μm in the polymeric approach.

4.3. Beneficial Properties of DDL Electrodes with Microdistancing

The relatively high reactive species concentrations, produced in a low conductive electrolyte during this study, can be explained by the electrode setup itself. The maximum distance depended on the thickness of the DDL and the inner diameter of the steel cannula (see Figure 7). The minimum spacing between anode and cathode can be equated with the thickness of the non-conductive UDD layer. The spacing of a few micrometers between anode and cathode gave the DDL a unique position in the world of electrode setups. The scale of the electrode gap in the DDL concept is only comparable to integrated double diamond electrodes [19] or microelectrode arrays [26,30]. In classical electrode setups, the spacing between anode and cathode varies from several hundred micrometers up to multiple centimeters. The reduction in the gap to a micrometer scale correlated directly with the voltage required to cause a desired electrochemical reaction. This, in fact, means that EAOPs can also take place in poorly conductive electrolytes (e.g., demineralized water) at reasonable voltages (5–15 V) while producing oxidative species, which is indicated by hydrogen-peroxide test strips.

Assuming that 100% of the wire's surface is electrochemically active, the minimum current density is equal to 0.01 A/cm^2 (at 5 V). The current density for BDD-based systems for wastewater treatment or the specific removal of bacteria in the literature is within the range of 0.01–0.1 A/cm^2 [31–33].

5. Conclusions and Outlook

The coexistence of conductive and non-conductive diamond, at the micrometer level, enables the use of BDD as an in situ disinfection tool at the smallest possible scale. The electrical insulation provided by the UDD eliminates the need for a polymeric alternative with all its drawbacks (large thickness, byproducts, detachment). Manufacturing the DDL currently requires multiple manual steps, but the above-described procedure could serve as the basis for an industrial production. Further work has to be carried out in order to show how robust and operational the concept is, but the first results look promising. Rinsing an electrolyte through a steel cannula while electrochemical activating it with a DDL demonstrated significant oxidant production, regardless of the conductivity of the electrolyte. Going forwards, the concentrations of various oxidation products must be determined and their disinfecting potential studied in microbiological tests. A mechanical and chemical comparison between the polymer-based approach versus the DDL concept is the new objective.

6. Patents

A.B., M.Ka. and S.R. filed a patent (EP 3733238 B1) for the electrochemical disinfection method described in this report.

References

1. Nidheesh, P.V.; Divyapriya, G.; Oturan, N.; Trellu, C.; Oturan, M.A. Environmental applications of boron-doped diamond electrodes: 1. Applications in water and wastewater treatment. *ChemElectroChem* **2019**, *6*, 2124. [CrossRef]

2. Ochiai, T.; Iizuka, Y.; Nakata, K.; Murakami, T.; Tryk, D.A.; Fujishima, A.; Koide, Y.; Morito, Y. Efficient electrochemical decomposition of perfluorocarboxylic acids by the use of a boron-doped diamond electrode. *Diam. Relat. Mater.* **2011**, *20*, 64–67. [CrossRef]

3. Schorr, B.; Ghanem, H.; Rosiwal, S.; Geißdörfer, W.; Burkovski, A. Elimination of bacterial contaminations by treatment of water with boron-doped diamond electrodes. *World J. Microbiol. Biotechnol.* **2019**, *35*, 48. [CrossRef]

4. Davis, J.; Baygents, J.C.; Farrell, J. Understanding persulfate production at boron doped diamond film anodes. *Electrochim. Acta* **2014**, *150*, 68–74. [CrossRef]

5. Divyapriya, G.; Nidheesh, P.V. Electrochemically generated sulfate radicals by boron doped diamond and its environmental applications. *Curr. Opin. Solid State Mater. Sci.* **2021**, *25*, 100921. [CrossRef]

6. Griesbach, U.; Malkowsky, I.M.; Waldvogel, S.R. Green electroorganic synthesis using BDD electrodes. In *Electrochemistry for the Environment*; Comninellis, C., Chen, G., Eds.; Springer: New York, NY, USA, 2010; pp. 125–141.

7. Lips, S.; Waldvogel, S.R. Use of boron-doped diamond electrodes in electro-organic synthesis. *ChemElectroChem* **2019**, *6*, 1649–1660. [CrossRef]

8. Waldvogel, S.R.; Mentizi, S.; Kirste, A. Boron-doped diamond electrodes for electroorganic chemistry. In *Topics in Current Chemistry*; Springer: Berlin/Heidelberg, Germany, 2012; Volume 320, pp. 1–32.

9. Zhang, F.; Sun, Z.; Cui, J. Research on the mechanism and reaction conditions of electrochemical preparation of persulfate in a split-cell reactor using BDD anode. *RSC Adv.* **2020**, *10*, 33928–33936. [CrossRef]

10. Tago, S.; Ochiai, T.; Suzuki, S.; Hayashi, M.; Kondo, T.; Fujishima, A. Flexible boron-doped diamond (BDD) electrodes for plant monitoring. *Sensors* **2017**, *17*, 1638. [CrossRef]

11. Dwyer, D.J.; Kohanski, M.A.; Collins, J.J. Role of reactive oxygen species in antibiotic action and resistance. *Curr. Opin. Microbiol.* **2009**, *12*, 482–489. [CrossRef] [PubMed]

12. Koch, M.; Rosiwal, S.; Burkovski, A. Environmentally sustainable elimination of microbes using boron-doped diamond electrodes. In *Microbial Biotechnology*; Chowdhary, P., Mani, S., Chaturvedi, P., Eds.; Wiley: Weinheim, Germany, 2022; pp. 355–364.

13. Böhm, A.L.; Koch, M.; Rosiwal, S.; Burkovski, A.; Karl, M.; Grobecker-Karl, T. Electrochemical disinfection of experimentally infected teeth by boron-doped diamond electrode treatment. *J. Clin. Med.* **2019**, *8*, 2037. [CrossRef] [PubMed]

14. Göltz, M.; Koch, M.; Detsch, R.; Karl, M.; Burkovski, A.; Rosiwal, S. Influence of in-situ electrochemical oxidation on implant surface and colonizing microorganisms evaluated by scanning electron microscopy. *Materials* **2019**, *12*, 3977. [CrossRef] [PubMed]

15. Klär, V.; Palarie, V.; Burkovski, A.; Karl, M.; Grobecker-Karl, T. Pilot study on the applicability of boron-doped diamond electrodes for tooth whitening. *Clin. Exp. Dent. Res.* **2022**, *8*, 757–762. [CrossRef]

16. Koch, M.; Palarie, V.; Göltz, M.; Kurzer, M.; Zulla, M.; Rosiwal, S.; Willner, M.; Burkovski, A.; Karl, M. Root canal obturation by electrochemical precipitation of calcium phosphates. *Appl. Sci.* **2022**, *12*, 2956. [CrossRef]

17. Koch, M.; Palarie, V.; Koch, L.; Burkovski, A.; Zulla, M.; Rosiwal, S.; Karl, M. Preclinical testing of boron-doped diamond electrodes for root canal disinfection: A series of preliminary studies. *Microorganisms* **2022**, *10*, 782. [CrossRef]

18. Koch, M.; Göltz, M.; Xiangjun, M.; Karl, M.; Rosiwal, S.; Burkovski, A. Electrochemical disinfection of dental implants experimentally contaminated with microorganisms as a model for periimplantitis. *J. Clin. Med.* **2020**, *9*, 475. [CrossRef] [PubMed]

19. Koch, M.; Burkovski, A.; Zulla, M.; Rosiwal, S.; Geißdörfer, W.; Dittmar, R.; Grobecker-Karl, T. Pilot study on the use of a laser-structured double diamond electrode (DDE) for biofilm removal from dental implant surfaces. *J. Clin. Med.* **2020**, *9*, 3036. [CrossRef] [PubMed]

20. Ochiai, T.; Ishii, Y.; Tago, S.; Hara, M.; Sato, T.; Hirota, K.; Nakata, K.; Murakami, T.; Einaga, Y.; Fujishima, A. Application of boron-doped diamond microelectrodes for dental treatment with pinpoint ozone-water production. *ChemPhysChem* **2013**, *14*, 2094–2096. [CrossRef]

21. May, P.W.; Rego, C.A.; Thomas, R.M.; Ashfold, M.N.R.; Rosser, K.N.; Everitt, N.M. CVD diamond wires and tubes. *Diam. Relat. Mater.* **1994**, *3*, 810–813. [CrossRef]

22. Manfredotti, C.; Fizzotti, F.; Lo Giudice, A.; Mucera, G.; Polesello, P.; Vittone, E.; Mankelevich, Y.A.; Suetin, N.V. Growth and characterisation of CVD diamond wires for X-ray detection. *Diam. Relat. Mater.* **1997**, *6*, 1051–1056. [CrossRef]

23. Abada, H.M.; Hashem, A.A.R.; Abu-Seida, A.M.; Nagy, M.M. The effect of changing apical foramen diameter on regenerative potential of mature teeth with necrotic pulp and apical periodontitis. *Clin. Oral. Investig.* **2022**, *26*, 1843–1853. [CrossRef] [PubMed]

24. Asai, K.; Einaga, Y. Fabrication of an all-diamond microelectrode using a chromium mask. *Chem. Commun.* **2019**, *55*, 897–900. [CrossRef]

25. Holt, K.B. Diamond ultramicroelectrodes and nanostructured electrodes. In *Synthetic Diamond Films: Preparation, Electrochemistry, Characterization and Applications*; Brillas, E., Martinez-Huitle, C.A., Eds.; John Wiley: Hoboken, NJ, USA, 2011; p. 133.

26. Pagels, M.; Hall, C.E.; Lawrence, N.S.; Meredith, A.; Jones, T.G.J.; Godfried, H.P.; Pickles, C.S.J.; Wilman, J.; Banks, C.E.; Compton, R.G.; et al. All-diamond microelectrode array device. *Anal. Chem.* **2005**, *77*, 3705–3708. [CrossRef]

27. Einaga, Y. Boron-doped diamond electrodes: Fundamentals for electrochemical applications. *Acc. Chem. Res.* **2022**, *55*, 3605–3615. [CrossRef]

28. McBeath, S.T.; Wilkinson, D.P.; Graham, N.J.D. Application of boron-doped diamond electrodes for the anodic oxidation of pesticide micropollutants in a water treatment process: A critical review. *Environ. Sci. Water Res. Technol.* **2019**, *5*, 2090–2107. [CrossRef]

29. Borchardt, R.; Sand, P.; Fromm, T.; Rosiwal, S. Novel structuring technique for diamond coatings. *Diam. Relat. Mater.* **2020**, *110*, 108103. [CrossRef]

30. Didier, C.M.; Kundu, A.; Deroo, D.; Rajaraman, S. Development of in vitro 2D and 3D microelectrode arrays and their role in advancing biomedical research. *J. Micromech. Microeng.* **2020**, *30*, 103001. [CrossRef]

31. Martínez-Huitle, C.A.; Brillas, E. A critical review over the electrochemical disinfection of bacteria in synthetic and real wastewaters using a boron-doped diamond anode. *Curr. Opin. Solid State Mater. Sci.* **2021**, *25*, 100926. [CrossRef]

32. Long, Y.; Ni, J.; Wang, Z. Subcellular mechanism of Escherichia coli inactivation during electrochemical disinfection with boron-doped diamond anode: A comparative study of three electrolytes. *Water Res.* **2015**, *84*, 198–206. [CrossRef]

33. Jeong, J.; Kim, J.Y.; Yoon, J. The role of reactive oxygen species in the electrochemical inactivation of microorganisms. *Environ. Sci. Technol.* **2006**, *40*, 6117–6122. [CrossRef]